


ORIGINAL ARTICLE

Open Access



Intra- and peri-tumoral MRI radiomics features for preoperative lymph node metastasis prediction in early-stage cervical cancer

Zhenhua Zhang^{1†}, Xiaojie Wan^{2†}, Xiyao Lei³, Yibo Wu³, Ji Zhang³, Yao Ai³, Bing Yu³, Xinmiao Liu⁴, Juebin Jin⁵, Congying Xie^{6*} and Xiance Jin^{3,7*} 

Abstract

Background Noninvasive and accurate prediction of lymph node metastasis (LNM) is very important for patients with early-stage cervical cancer (ECC). Our study aimed to investigate the accuracy and sensitivity of radiomics models with features extracted from both intra- and peritumoral regions in magnetic resonance imaging (MRI) with T2 weighted imaging (T2WI) and diffusion weighted imaging (DWI) for predicting LNM.

Methods A total of 247 ECC patients with confirmed lymph node status were enrolled retrospectively and randomly divided into training ($n = 172$) and testing sets ($n = 75$). Radiomics features were extracted from both intra- and peritumoral regions with different expansion dimensions (3, 5, and 7 mm) in T2WI and DWI. Radiomics signature and combined radiomics models were constructed with selected features. A nomogram was also constructed by combining radiomics model with clinical factors for predicting LNM.

Results The area under curves (AUCs) of radiomics signature with features from tumors in T2WI and DWI were 0.841 vs. 0.791 and 0.820 vs. 0.771 in the training and testing sets, respectively. Combining radiomics features from tumors in the T2WI, DWI and peritumoral 3 mm expansion in T2WI achieved the best performance with an AUC of 0.868 and 0.846 in the training and testing sets, respectively. A nomogram combining age and maximum tumor diameter (MTD) with radiomics signature achieved a C-index of 0.884 in the prediction of LNM for ECC.

Conclusions Radiomics features extracted from both intra- and peritumoral regions in T2WI and DWI are feasible and promising for the preoperative prediction of LNM for patients with ECC.

Key points

1. Radiomics models with features from MRI for LNM prediction for ECC.
2. Combined radiomics signature with intra- and peritumoral regions achieved the best performance.

[†]Zhenhua Zhang and Xiaojie Wan have contributed equally to this work.

*Correspondence:

Congying Xie
wzxiecongying@163.com
Xiance Jin
jinxc1979@hotmail.com

Full list of author information is available at the end of the article

3. Combined radiomics signature with an AUC of 0.846 for predicting LNM.
4. A nomogram combining clinical factors with radiomics signature further improves predictive performance.

Keywords Early-stage cervical cancer, Lymph nodes metastasis, Radiomics, Magnetic resonance imaging, Peritumoral region

Background

Although the incidence of cervical cancer (CC) in the developed countries has decreased for the past two decades, it remains the fourth most common cancer and the leading cause of cancer-related death worldwide in women [1]. Radical hysterectomy and pelvic lymphadenectomy are the standard treatment options for patients with early-stage cervical cancer (ECC) [2]. However, studies demonstrated that there is less than 30% ECC with pelvic lymph node metastasis (LNM), which indicates over 70% patients with ECC were over-treated and suffered from unnecessary complications of lymphadenectomy [3, 4]. It is necessary to identify LNM accurately for patients with ECC in order to avoid unnecessary lymphadenectomy. Sentinel lymph node (SLN) biopsy has been suggested to decrease the need of pelvic lymphadenectomy for patients with ECC [5, 6]. The accuracy of SLN biopsy can be improved by several types of ancillary methods, including immunohistochemistry, polymerase chain reaction and serial sectioning [5–8]. However, both lymphadenectomy and SLN biopsy are invasive modalities; therefore, noninvasive and accurate prediction of LNM is very important for patients with ECC.

Magnetic resonance imaging (MRI) is the mainstay image modality for the staging of CC, especially the apparent diffusion coefficient (ADC) values derived from diffusion weighted imaging (DWI) are increasing applied to characterize the tumor microenvironment and microstructure of CC for LNM diagnosis [9]. However, traditional MRI mainly assesses the sizes of lymph nodes and is limited in its diagnosis sensitivity, which may lead to inappropriate treatment decisions [10]. With the emergence of radiomics, many attempts had been reported using different combinations of MRI in the preoperative prediction of LNM for patients with CC, such as T2 weighted imaging sequences (T2WI) [11–13], T2WI combined with dynamic contrast-enhanced MRI (DCE) [14–16], multiple-parameters MRI [17–19], ADC [20], as well as T2WI combined with ADC for locally advanced CC [21]. Although the sensitivity of MRI in the prediction of LNM has been improved with radiomics, the overall performance of these studies ranged from poor to moderate, particularly, radiomics features extracted from lymph nodes

rather than primary tumor in some studies may affect the stability of radiomics features resulting from the relatively small volume of lymph nodes [22].

The purpose of this study is to investigate the accuracy and sensitivity of intra- and peritumoral radiomics features in T2WI, DWI sequences for preoperative LNM prediction with ECC patients and develop a flexible nomogram with clinical factors for potential clinical utilities.

Materials and methods

Patients

Patients with ECC from January 2008 and December 2018 were retrospectively reviewed and analyzed through searching electronic medical records in the authors' hospital. The inclusion criteria were: (1) patients underwent radical hysterectomy and systematic pelvic lymph node dissection; (2) with histologically confirmed ECC according to the International Federation of Gynecology and Obstetrics (FIGO) stage; (3) without any treatment before surgery; (4) with detailed clinical and pathological characteristic; (5) standard MRI examination less than 2 weeks before hysterectomy. The exclusion criteria were: (1) incomplete clinical data; (2) lack of sufficient MRI sequences: T2WI with fat suppression or DWI; (3) poor image quality (including artifacts and the slices of ROI < 3 slices) [14]. The patients' selection flowchart is shown in Fig. 1. The Ethics Committee in Clinical Research (ECCR) of the authors' hospital approved this study, which was conducted in accordance with the Declaration of Helsinki (ECCR no. 2019059), and waived the need of written informed consent with confirmation of patient data confidentiality due to nature of the retrospective study.

MRI acquisition and segmentation

MR images of sagittal T2WI with fat suppression and transverse DWI were acquired through a 3.0 T scanner (PHILIPS, ACHIEVA) using a 16-channel phased array body coil. T2WI was acquired applying parameters of TR/TE = 3000/90 ms, FOV = 220 × 220 mm, matrix = 336 × 336, thickness = 4 mm and gap = 1 mm with fast spin echo sequence. DWI was acquired applying parameters of TR/TE = 3000/55 ms, FOV = 430 × 334 mm, matrix = 224 × 224, thickness = 4 mm, and gap = 1 mm in transverse orientation

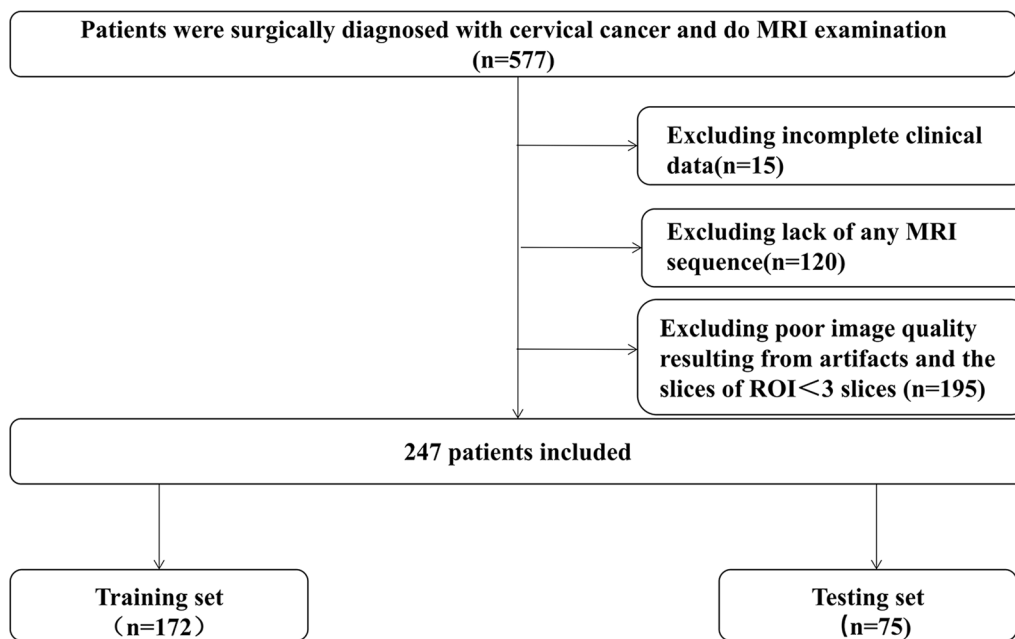


Fig. 1 The flowchart for patients recruitment in this study

including the entire female pelvis with a single-shot echo planar imaging (EPI) sequence using a b value of 0 and 1000 s/mm^2 . All images were stored in a picture archiving and communication system (PACS).

The regions of interest (ROIs) of tumor were manually delineated along the boundary of the tumor slice by slice in sagittal T2WI with fat suppression and transverse DWI by a radiologist with 7 years of experience via a 3D Slicer software (version 4.2.1, <https://www.slicer.org>). A mask of the area with tumor boundary was defined as the intra-tumoral region. The peritumoral ROIs were obtained with python (version 3.7.6) by uniform expansion of intra-tumoral region with a dimension of 3 mm, 5 mm, 7 mm, respectively [23, 24]. The tumor boundary to the outer expansion boundary was defined as peritumoral region. In order to ensure the accuracy of segmentation, in the process of image segmentation, a senior radiologist has already validated all uncertain segmentation. Typical ROIs of intra- and peritumoral regions in sagittal T2WI with fat suppression and transverse DWI are shown in Fig. 2.

Radiomics feature extraction and selection

In preprocessing, intensity normalization was performed to transform arbitrary gray intensity values into a standardized intensity range in T2WI and DWI. Radiomics features of first-order, shape-based, texture, Laplacian of Gaussian and wavelet features were extracted from contoured intra- and peritumoral ROIs using Python package (Pyradiomics) according to Image Biomarker

Standardization Initiative (IBSI) [25]. Mann–Whitney U tests were firstly used to select potentially informative features with a $p < 0.05$. Secondly, the least absolute shrinkage and selection operator (LASSO) method was applied to select the optimal features through tuning the coefficient λ and using ten-fold cross-validation to avoid over-fitting.

Radiomics signature and nomogram

Radiomics signatures were constructed with selected optimal features and their nonzero coefficients from intra- and peritumoral ROIs, as well as their combinations for the prediction of LNM status. The performance of radiomics signatures was evaluated by receiver operating characteristic (ROC) curves and the value of area under curve (AUC). Univariate analysis was performed to select clinical factors that associated with LNM of ECC. A nomogram was constructed using multivariate logistic regression integrating clinical factors and radiomics signature for the preoperatively prediction of LNM of ECC. A C-index was calculated in the training and testing sets to assess the discrimination performance of the nomogram. Calibration curves were plotted to evaluate the calibration of the radiomics nomogram with 1000 bootstrap resamples, and the goodness of fit was assessed with the Hosmer–Lemeshow (H–L) test [26].

Statistics analysis

Statistical analyses were performed in R software (version 3.6.0, <http://www.Rproject.org>). Key radiomics features

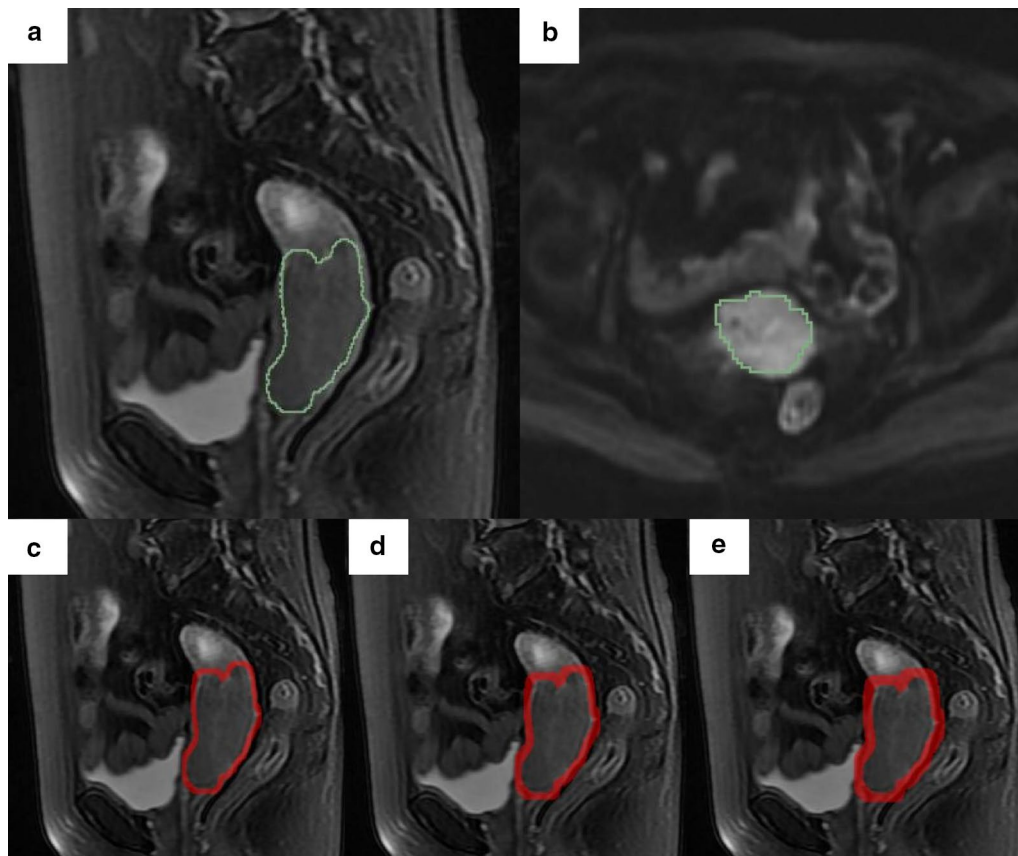


Fig. 2 The intra- and peritumoral ROIs in this study. **a** is on sagittal T2WI; **b** is on DWI. The green line represents the boundary of the tumor; **c–e** are the example (3, 5, 7 mm expansion dimension) of the dilated MRI with various radial dilation distances outside the original masks in the MRI. The red rings indicate the peritumoral regions

selection and logistic regression modeling were done using the “glmnet” package. Nomogram construction and calibration plots were performed using “rms” package. The H–L test was performed using “Resource Selection” package. The ROC curves were calculated using Medcalc software. For continuous clinical variables, two sample t test was used to assess the equality of variances between positive and negative LNM groups. For categorical variables, fisher’s exact test and Chi-square test were used to test the difference between groups. For all tests, $p < 0.05$ was considered as statistically significant.

Results

A total of 247 patients with ECC were enrolled in this study with a mean age of 54.1 ± 10.01 (range, 28–77), as shown in Fig. 1 for the patients enrollment. There were 79 patients with LNM and 168 of non-LNM, respectively. Patients were randomly divided into training and testing sets by a ratio of 7 to 3 with 172 patients (mean age \pm SD, 53.91 ± 9.88 ; range, 28–77) and 75 patients (mean age \pm SD, 54.54 ± 10.35 ; range, 30–75) allocated to

the training and testing sets, respectively. There was no significant difference in LNM status between the training and testing sets (31.9% vs. 32%, $p = 0.92$). Detailed clinicopathologic characteristics of patients are shown in Table 1.

A total of 1014 radiomics features were extracted from the intra-, peritumoral ROIs with 3 mm, 5 mm and 7 mm expansion in T2WI and DWI, respectively. After Mann–Whitney U test, there were 676, 442, 409, 462 and 645, 387, 298, 285 radiomics features that were selected with intra-, peritumoral ROIs with 3 mm, 5 mm, and 7 mm expansion in T2WI and DWI. By applying LASSO method, a total of 17, 12, 12, 12 and 9, 15, 5, 11 optimal radiomics features were remained, respectively. The details are shown in Additional file 1: Fig. S1. Additional file 1: Table S1 shows the selected radiomics features and their corresponding nonzero coefficients. Radiomics score (Radscore) was calculated by multiplying the features with their corresponding nonzero coefficients and then adding them together. The Radscore based on intra-, peritumoral ROIs with 3 mm, 5 mm, and 7 mm

Table 1 Characteristics of the enrolled patients in the training and testing sets

Characteristic	Training set (n = 172)		p	Testing set (n = 75)		p
	LNM (n = 55)	Non-LNM (n = 117)		LNM (n = 24)	Non-LNM (n = 51)	
Age (mean ± SD)			0.083			0.64
Mean	51.80	54.91		55.54	54.04	
SD	11.68	8.79		10.77	10.23	
FIGO stage			0.69			0.64
I	25 (45.45%)	57 (48.72%)		9 (37.5%)	22 (43.14%)	
II	30 (54.55%)	60 (51.28%)		15 (62.5%)	29 (56.86%)	
Pathological type			0.95			0.086
SCC	46 (83.64%)	99 (84.61%)		20 (83.34%)	43 (84.31%)	
AC	5 (9.09%)	8 (6.84%)		2 (8.33%)	8 (15.69%)	
Others	4 (7.27%)	10 (8.55%)		2 (8.33%)		
MTD			0.016			0.009
≤ 4 cm	36 (65.45%)	96 (82.05%)		15 (62.50%)	45 (88.24%)	
> 4 cm	19 (34.55%)	21 (17.95%)		9 (37.50%)	6 (11.76%)	
LVSI			< 0.001			0.01
Negative	27 (49.09%)	91 (77.78%)		13 (54.17%)	42 (82.35%)	
Positive	28 (50.91%)	26 (22.22%)		11 (45.83%)	9 (17.65%)	

LNM: lymph node metastasis; Non-LNM: without lymph node metastasis; SD: standard deviation; FIGO: International Federation of Gynecology and Obstetrics; MTD: maximum tumor diameter; SCC: Squamous cell carcinoma; AC: Adenocarcinoma; LVSI: lymph-vascular space invasion

expansion in T2WI and DWI for each patient is shown in Additional file 1: Fig. S2.

The AUCs of radiomics signature with features from tumors in T2WI and DWI were 0.841 (0.779–0.904) vs. 0.791 (0.718–0.865) and 0.820 (0.715–0.926) vs. 0.771 (0.664–0.879) in the training and testing sets, respectively. The best performance of radiomics signature with features extracted from peritumoral ROIs was peritumoral 3 mm expansion in T2WI and DWI with an AUC of 0.786 (0.669–0.903) and 0.734 (0.623–0.846) in the testing sets, respectively. Combining radiomics with features from tumor and peritumoral expansion achieved a best AUC of 0.837 (0.733–0.940) and 0.768 (0.659–0.877) in the testing set for tumor plus peritumoral 3 mm expansion in the T2WI and DWI, respectively. Combined radiomics signature from tumors in the T2WI, DWI and peritumoral 3 mm expansion in T2WI achieved an AUC of 0.868 (0.809–0.915) and 0.846 (0.753–0.940) in the training and testing sets, respectively. Detailed performance of these models is presented in Table 2 and Fig. 3.

As shown in Table 3, the univariate analysis of clinical factors that associated with LNM of ECC, age and MTD were selected and combined with radiomics signature to develop a nomogram using multivariate logistic regression to further improve the prediction on the LNM status for ECC. The lymph-vascular space invasion (LVSI) was not included as it can be obtained only postoperatively. As shown in Fig. 4a, the nomogram achieved a C-index of 0.884 (95% CI, 0.831–0.937) in the prediction of LNM

for patients with ECC. The calibration curves are shown in Fig. 4b, c with no statistical significance observed in the H–L test ($p = 0.55$ and $p = 0.14$).

Discussion

In this study, radiomics features extracted from the tumor regions in T2WI and DWI achieved an AUC of 0.820 and 0.771, respectively, in the prediction of LNM for patients with ECC. Combined features from tumor regions with additional features extracted from peritumoral 3 mm expansion in T2WI improved the AUC to 0.846 in the LNM prediction. A C-index of 0.884 was achieved with a nomogram integrating combined radiomics signature with clinical factors in the prediction of LNM for patients with ECC.

LNM is one of the most important prognostic factors for patients with ECC with a reported 5-year survival rate of 55% vs. 90% for patients with vs. without LNM [27]. LNM is also important evidence for treatment decision with chemoradiation rather than surgery as their first choice to avoid possible serious complications [28]. In this study, 79 (31.9%) of the enrolled 247 patients were confirmed with LNM, which is a bit higher than reported statistics of less than 30% of ECC with LNM [28]. This may be due to that 134 out of 247 ECC patients (54.24%) enrolled in this study were of FIGO stage II or patients selection bias due to a large number of patients excluded because of image quality or incomplete MRI sequences. Therefore, accurately identifying the LNM preoperatively

Table 2 Performance of radiomics signature with features extracted from tumor and peritumoral regions of interest

Models	Training sets				Testing sets			
	AUC (95% CI)	ACC	SEN	SPE	AUC (95% CI)	ACC	SEN	SPE
T2WI								
Tumor	0.841 (0.779–0.904)	0.791	0.778	0.818	0.820 (0.715–0.926)	0.760	0.706	0.875
Peritumoral 3 mm	0.775 (0.702–0.847)	0.733	0.684	0.836	0.786 (0.669–0.903)	0.720	0.647	0.875
Peritumoral 5 mm	0.795 (0.724–0.866)	0.762	0.761	0.764	0.783 (0.664–0.903)	0.720	0.783	0.833
Peritumoral 7 mm	0.795 (0.727–0.862)	0.762	0.798	0.680	0.755 (0.624–0.886)	0.787	0.898	0.577
DWI								
Tumor	0.791 (0.718–0.865)	0.773	0.829	0.650	0.771 (0.664–0.879)	0.680	0.608	0.833
Peritumoral 3 mm	0.810 (0.743–0.876)	0.738	0.727	0.764	0.734 (0.623–0.846)	0.613	0.451	0.958
Peritumoral 5 mm	0.745 (0.666–0.825)	0.750	0.812	0.618	0.725 (0.605–0.844)	0.600	0.451	0.917
Peritumoral 7 mm	0.803 (0.733–0.873)	0.720	0.65	0.873	0.696 (0.567–0.826)	0.720	0.725	0.708
T + 3 mm T2WI	0.851 (0.790–0.912)	0.797	0.795	0.800	0.837 (0.733–0.940)	0.813	0.784	0.875
T + 5 mm T2WI	0.865 (0.807–0.923)	0.780	0.701	0.945	0.818 (0.710–0.926)	0.733	0.647	0.917
T + 7 mm T2WI	0.830 (0.765–0.896)	0.750	0.667	0.927	0.811 (0.702–0.921)	0.747	0.706	0.833
T + 3 mm DWI	0.784 (0.710–0.860)	0.744	0.752	0.727	0.768 (0.659–0.877)	0.693	0.627	0.833
T + 5 mm DWI	0.781 (0.705–0.856)	0.721	0.786	0.691	0.767 (0.657–0.877)	0.707	0.647	0.833
T + 7 mm DWI	0.779 (0.703–0.855)	0.750	0.761	0.727	0.765 (0.655–0.874)	0.707	0.647	0.833
T (T2WI) + T(DWI)	0.867 (0.810–0.924)	0.802	0.829	0.746	0.836 (0.741–0.931)	0.760	0.706	0.875
T + T + 3 mm T2WI	0.868 (0.809–0.915)	0.800	0.803	0.817	0.846 (0.753–0.940)	0.808	0.784	0.833

T2WI: T2 weighted imaging; DWI: diffusion-weighted imaging; AUC: area under curve; ACC: accuracy; SEN: sensitivity; SPE: specificity; T + xmm: tumor plus peritumoral x mm expansion;

is of critical clinical importance in the management of patients with ECC.

T2WI, contrast-enhanced TIWI and DWI have long been applied for the diagnosis of LNM with a relatively low sensitivity of 38%–56% reported [29, 30]. In this study, the sensitivity for LNM prediction was improved from 0.647 to 0.898, and 0.451 to 0.725 for radiomics models with features from T2WI and DWI in the testing, respectively. Models with combined features from tumor and peritumoral regions did not improve the sensitivity in this study. This is inconsistent with the study of Wu et al. [21] in which the sensitivity was increased from 43% to 85.7% for models with features extracted from tumor or peritumoral regions alone compared with models with combined tumor and peritumoral regions features in T2WI. For features extracted from DWI, the combined model showed a worse sensitivity compared with models with features extracted from tumor or peritumoral regions. This may be due to the differences in the definition of peritumoral regions between two studies. Automatic expansion with 3–7 mm margin was applied in this study, instead of a manual segmentation of peritumoral regions in the study of Wu et al. [21].

In this study, the AUCs of radiomics model with features extracted from tumors in the T2WI and DWI were 0.841, 0.791 and 0.820, 0.771 in the training and testing sets, respectively. This is higher than reported AUC of

0.763, 0.829 and 0.699, 0.613 in the training and validation sets with T2WI and ADC, respectively, in the study of Hou et al. [17] for the prediction of LNM for ECC. Combined T2WI and DWI model in this study achieved an AUC of 0.836 in the testing sets which is close to the reported AUC of 0.833 with combined T2WI, ADC and contrast-enhanced T1WI in the study of Hou et al. [31]. However, Yu et al. [20] demonstrated that radiomics features extracted from ADC maps alone were able to achieve an AUC of 0.870 in the predicting of LNM for early-stage cervical squamous cell carcinoma. This indicated that radiomics features extracted from DWI and ADC maps revealed different messages although ADC maps were calculated from DWI and the selection of b-values may significantly affect texture analysis on DWI images [31].

The radiomics models with features extracted from peritumoral regions in T2WI and DWI also demonstrated reasonable an AUC from 0.755 to 0.786, and from 0.696 to 0.734 in the testing sets, respectively. This indicated that peritumoral regions may hold information regarding the LNM status as pointed out that tumor cells tend to migrate from the primary tumor to the peritumoral regions and lead to morphological changes in MRI [32]. However, the prediction performance did not improve with increasing peritumoral region and the peritumoral 3 mm in T2WI and DWI achieved the highest prediction

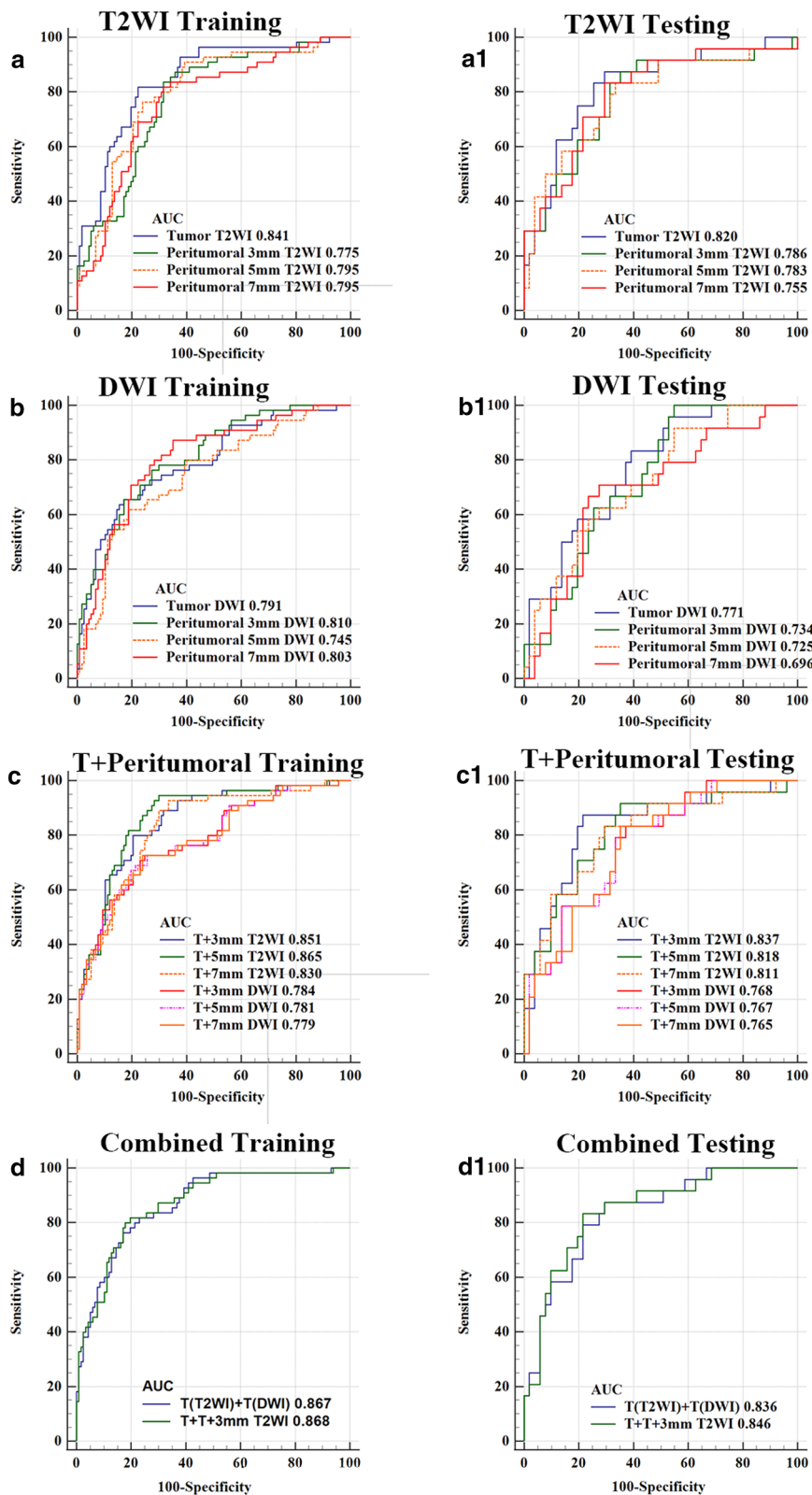


Fig. 3 ROC curves of intra- and peritumoral regions with (3, 5, 7 mm) expansion dimension, intra-tumoral region plus peritumoral regions with (3, 5, 7 mm) expansion dimension on T2WI and DWI, combining intra-tumor regions in T2WI and DWI, combined radiomics signature from tumors in the T2WI, DWI and peritumoral 3 mm expansion in T2WI in the (a-d) training and (a1-d1) testing sets, respectively

Table 3 Univariate analysis of clinical factors that were associated with lymph node metastasis

Variables	Odds ratios	95% confident interval	<i>p</i>
Age	0.968	0.936–1.001	0.056
FIGO stage	1.140	0.599–2.168	0.69
Pathological type	0.996	0.608–1.631	0.99
MTD	2.413	1.164–5.003	0.018
LVSI	3.630	1.829–7.201	<0.001

FIGO: International Federation of Gynaecology and Obstetrics; MTD: maximum tumor diameter; LVSI: lymph-vascular space invasion

performance, which may suggest that the increase in peritumoral region brings some irrelevant information; for example, the peritumoral 5 mm and 7 mm regions of

some FIGO II stage patients may contain other tissues affecting the prediction performance. Combined radiomics models with tumor and peritumoral 3 mm regions further improved the performance in both T2WI and DWI in this study with a highest AUC of 0.868 and 0.846 achieved in the training and testing sets, respectively. This is consistent with the study of Shi et al. [23] in which both intra- and peritumoral regions of contrast-enhanced T1WI and T2WI were combined to achieve an AUC of 0.830 and 0.853.

Radiomics nomogram with multi-parametric MRI, such as T1WI, T2WI, contrast-enhanced, DWI, and ADC, has been reported to achieve a good performance for LNM prediction with a C-index of 0.882 in the primary cohorts [18]. Similarly, the nomogram in this study

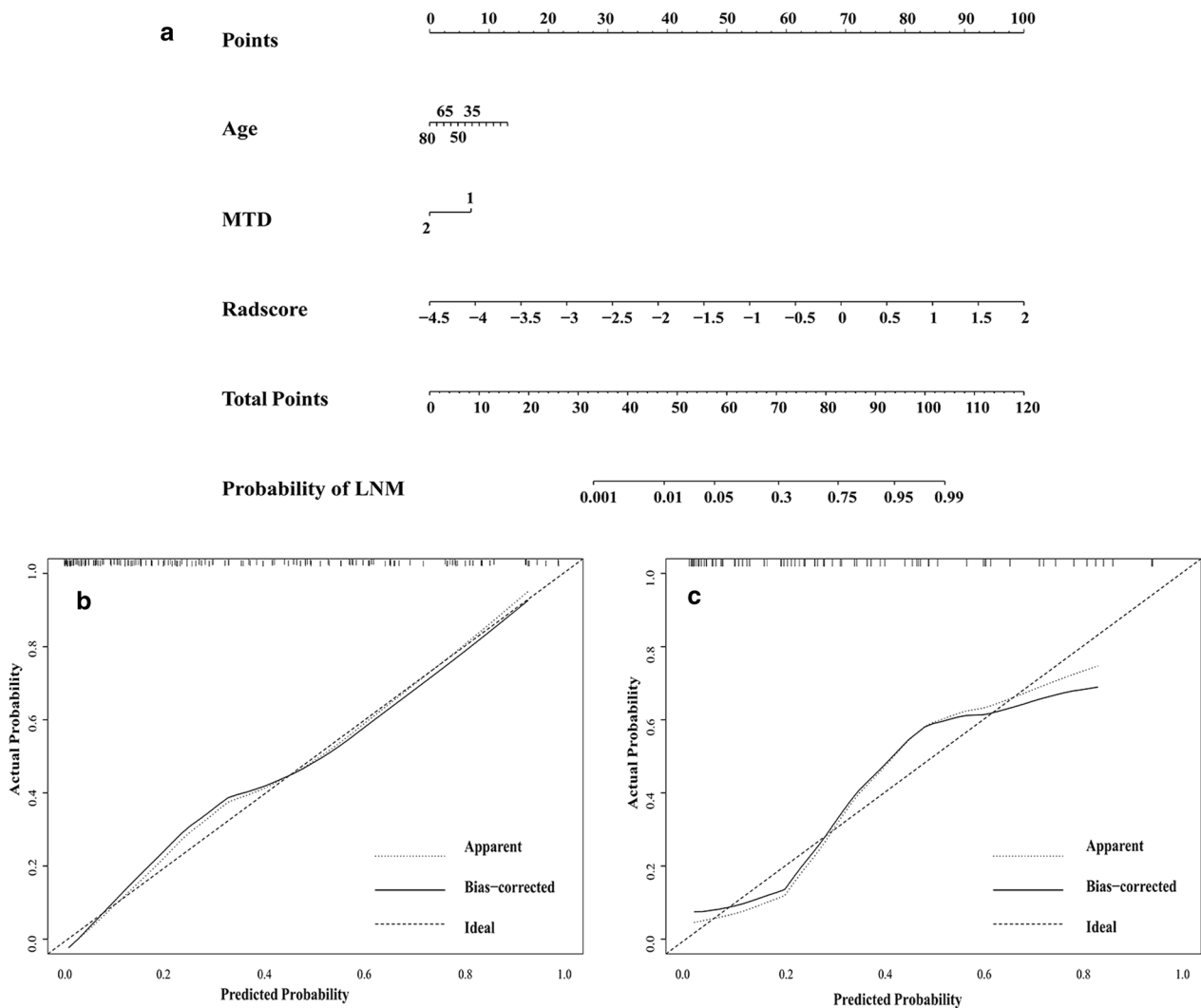


Fig. 4 Nomogram was developed by integrating the clinical factors (age and MTD) and combined radiomics signature in the training set (**a**); Calibration curve of the radiomics nomogram for predicting LNM in the (**b**) training set ($p=0.55$) and in the (**c**) testing set ($p=0.14$)

achieved a C-index of 0.884 and calibration curve analysis further confirmed the clinical usefulness of our nomogram for the preoperative LNM prediction. Except for MRI based radiomics, ultrasound images [33], ¹⁸F-fluorodeoxyglucose positron emission tomography/computed tomography (PET/CT) had also been investigated for the preoperative prediction of LNM for ECC [34]. Nomogram with radiomics features from multiple imaging modalities needs further investigation. Recently, deep learning models had also been investigated to predict the LNM of ECC to avoid time consuming target delineations in radiomics, whose clinical application and integration with radiomics worth further investigation [19].

The limitations of this study include that it is a retrospective study in single center, fewer patients recruited and lacking of the external validation may lead to overfitting of the models, larger sample size from multi-center is needed to improve the robust of the models; large number of patients excluded due to artifacts and incomplete MRI sequences may lead to bias in patients selection, and the scanning technique needs to be further improved and standardized; lacking of doing intraclass correlations coefficient analysis may affect the stability of feature selection and the robust of the model, and it will be improved in the following study; contrast-enhanced T1WI and ADC maps were not included in this work; automatic segmentation needs further investigation to improve the efficiency of radiomics study.

Conclusions

Radiomics features extracted from both intra- and peritumoral regions in T2WI and DWI are feasible and promising for the preoperative prediction of LNM for patients with ECC.

Abbreviations

AC	Adenocarcinoma
ADC	Apparent diffusion coefficient
AUC	Area under the curve
CC	Cervical cancer
DCE	Dynamic contrast enhanced
DWI	Diffusion weighted imaging
ECC	Early-stage cervical cancer
ECCR	Ethics committee in clinical research
EPI	Echo planar imaging
FIGO	International federation of gynecology and obstetrics
H-L	Hosmer–Lemeshow
IBSI	Image biomarker standardization initiative
LASSO	Least absolute shrinkage and selection operator
LNM	Lymph node metastasis
LVS	Lymph-vascular space invasion
MRI	Magnetic resonance imaging
MTD	Maximum tumor diameter
PACS	Picture archiving and communication system
PET/CT	Positron emission tomography/computed tomography
Radscore	Radiomics score
ROC	Receiver operating characteristic
ROIs	Regions of interest

SCC	Squamous cell carcinoma
SLN	Sentinel lymph node
T2WI	T2 weighted imaging

Supplementary Information

The online version contains supplementary material available at <https://doi.org/10.1186/s13244-023-01405-w>.

Additional file 1. Radiomic feature selection and the optimal features from different ROIs in T2WI and DWI; Radscores for each patient in the intra- and peritumoral regions with (3,5,7mm) expansion dimension on T2WI and DWI.

Author contributions

ZZ and XW contributed equally. XJ and CX were guarantors of integrity of the entire study and contributed to study concepts and design. ZZ and XW were involved in experimental studies, data analysis and manuscript editing. Other authors were involved in charting editing and data analysis supporting. All authors read and approved the final manuscript.

Funding

Partial of this work is supported by a funding from the key R&D project of the Department of Science and Technology of Zhejiang Province (2020C03028); the key project jointly built by the Provinces and Ministry of Zhejiang Health Commission (2021438235) and Major Project of Wenzhou Science and Technology Bureau (ZY2020011,ZY2022016).

Availability of data and material

The datasets used and/or analyzed during the current study are available from the corresponding author on reasonable request.

Declarations

Ethics approval and consent to participate

The Ethics Committee in Clinical Research (ECCR) of authors' hospital approved this study, which was conducted in accordance with the Declaration of Helsinki (ECCR no. 2019059), and waived the need of written informed consent with confirmation of patient data confidentiality due to nature of retrospective study.

Consent for publication

Not applicable.

Competing interests

The authors declare that they have no conflicts of interest.

Author details

¹Department of Radiology, The 1st Affiliated Hospital of Wenzhou Medical University, Wenzhou, China. ²Department of Obstetrics and Gynecology, Women's Hospital, Zhejiang University School of Medicine, Hangzhou, China. ³Department of Radiotherapy Center, The 1st Affiliated Hospital of Wenzhou Medical University, Wenzhou, China. ⁴School of Laboratory Medicine and Life Sciences, Wenzhou Medical University, Wenzhou, China. ⁵Department of Medical Engineering, The 1st Affiliated Hospital of Wenzhou Medical University, Wenzhou, China. ⁶Department of Radiation and Medical Oncology, The 2nd Affiliated Hospital of Wenzhou Medical University, Wenzhou, China. ⁷School of Basic Medical Science, Wenzhou Medical University, Wenzhou, China.

Received: 16 December 2022 Accepted: 16 March 2023

Published online: 15 April 2023

References

1. Ferlay J, SI, Ervik M, Dikshit R, Eser S, Mathers D, et al (2013) GLOBOCAN 2012 v1.0, Cancer Incidence and Mortality Worldwide: IARC CancerBase No. 11. Available via <http://globocan.iarc.fr>

2. Pecorelli S (2009) Revised FIGO staging for carcinoma of the vulva, cervix, and endometrium. *Int J Gynaecol Obstet* 105:103–104
3. Bats AS, Frati A, Mathevet P et al (2015) Contribution of lymphoscintigraphy to intraoperative sentinel lymph node detection in early cervical cancer: Analysis of the prospective multicenter SENTICOL cohort. *Gynecol Oncol* 137:264–269
4. Achouri A, Huchon C, Bats AS, Bensaid C, Nos C, Lecuru F (2013) Complications of lymphadenectomy for gynecologic cancer. *Eur J Surg Oncol* 39:81–86
5. Cormier B, Diaz JP, Shih K et al (2011) Establishing a sentinel lymph node mapping algorithm for the treatment of early cervical cancer. *Gynecol Oncol* 122:275–280
6. Lecuru F, Mathevet P, Querleu D et al (2011) Bilateral negative sentinel nodes accurately predict absence of lymph node metastasis in early cervical cancer: results of the SENTICOL study. *J Clin Oncol* 29:1686–1691
7. Bats AS, Mathevet P, Buenerd A et al (2013) The sentinel node technique detects unexpected drainage pathways and allows nodal ultrastaging in early cervical cancer: insights from the multicenter prospective SENTICOL study. *Ann Surg Oncol* 20:413–422
8. Kinkel K (2006) Pitfalls in staging uterine neoplasm with imaging: a review. *Abdom Imaging* 31:164–173
9. Balcacer P, Shergill A, Litkouhi B (2019) MRI of cervical cancer with a surgical perspective: staging, prognostic implications and pitfalls. *Abdom Radiol (NY)* 44:2557–2571
10. Choi HJ, Roh JW, Seo SS et al (2006) Comparison of the accuracy of magnetic resonance imaging and positron emission tomography/computed tomography in the presurgical detection of lymph node metastases in patients with uterine cervical carcinoma: a prospective study. *Cancer* 106:914–922
11. Zhou HL, Wen XL, Liu CY (2021) Value of T2WI-FS based radiomics features in the diagnosis of cervical cancer metastasis and lymph vascular space invasion. *Chin J Magn Reson Imaging* 12(07):69–71
12. Yan L, Yao H, Long R et al (2020) A preoperative radiomics model for the identification of lymph node metastasis in patients with early-stage cervical squamous cell carcinoma. *Br J Radiol* 93:20200358
13. Song J, Hu Q, Ma Z, Zhao M, Chen T, Shi H (2021) Feasibility of T2WI-MRI-based radiomics nomogram for predicting normal-sized pelvic lymph node metastasis in cervical cancer patients. *Eur Radiol* 31:6938–6948
14. Kan Y, Dong D, Zhang Y et al (2019) Radiomic signature as a predictive factor for lymph node metastasis in early-stage cervical cancer. *J Magn Reson Imaging* 49:304–310
15. Shijie DO, Xiaoxin HU, Wei WA, et al (2021) Prediction of lymph node metastasis of cervical cancer based on multi-sequence MRI and multi-system imaging omics mode. *China Oncol* 31:8
16. Deng X, Liu M, Sun J et al (2021) Feasibility of MRI-based radiomics features for predicting lymph node metastases and VEGF expression in cervical cancer. *Eur J Radiol* 134:109429
17. Hou L, Zhou W, Ren J et al (2020) Radiomics analysis of multiparametric MRI for the preoperative prediction of lymph node metastasis in cervical cancer. *Front Oncol* 10:1393
18. Xiao M, Ma F, Li Y et al (2020) Multiparametric MRI-based radiomics nomogram for predicting lymph node metastasis in early-stage cervical cancer. *J Magn Reson Imaging* 52:885–896
19. Wu Q, Wang S, Zhang S et al (2020) Development of a deep learning model to identify lymph node metastasis on magnetic resonance imaging in patients with cervical cancer. *JAMA Netw Open* 3:e2011625
20. Yu YY, Zhang R, Dong RT et al (2019) Feasibility of an ADC-based radiomics model for predicting pelvic lymph node metastases in patients with stage IB-IIA cervical squamous cell carcinoma. *Br J Radiol* 92:20180986
21. Wu Q, Wang S, Chen X et al (2019) Radiomics analysis of magnetic resonance imaging improves diagnostic performance of lymph node metastasis in patients with cervical cancer. *Radiother Oncol* 138:141–148
22. Li L, Zhang J, Zhe X et al (2022) A meta-analysis of MRI-based radiomic features for predicting lymph node metastasis in patients with cervical cancer. *Eur J Radiol* 151:110243
23. Shi J, Dong Y, Jiang W et al (2022) MRI-based peritumoral radiomics analysis for preoperative prediction of lymph node metastasis in early-stage cervical cancer: a multi-center study. *Magn Reson Imaging* 88:1–8
24. Cui L, Yu T, Kan Y, Dong Y, Luo Y, Jiang X (2022) Multi-parametric MRI-based peritumoral radiomics on prediction of lymph-vascular space invasion in early-stage cervical cancer. *Diagn Interv Radiol* 28:312–321
25. Zwanenburg A, Vallieres M, Abdalah MA et al (2020) The image biomarker standardization initiative: standardized quantitative radiomics for high-throughput image-based phenotyping. *Radiology* 295:328–338
26. Kramer AA, Zimmerman JE (2007) Assessing the calibration of mortality benchmarks in critical care: The Hosmer-Lemeshow test revisited. *Crit Care Med* 35:2052–2056
27. Gien LT, Covens FA (2010) Lymph node assessment in cervical cancer: prognostic and therapeutic implications. *J Surg Oncol* 99:242–247
28. Matsuura Y, Kawagoe T, Toki N, Tanaka M, Kashimura M (2006) Long-standing complications after treatment for cancer of the uterine cervix—clinical significance of medical examination at 5 years after treatment. *Int J Gynecol Cancer* 16:294–297
29. Cibula D, Zikan M, Slama J et al (2016) Risk of micrometastases in non-sentinel pelvic lymph nodes in cervical cancer. *Gynecol Oncol* 143:83–86
30. Wu Q, Zheng D, Shi L, Liu M, Wang M, Shi D (2017) Differentiating metastatic from nonmetastatic lymph nodes in cervical cancer patients using monoexponential, biexponential, and stretched exponential diffusion-weighted MR imaging. *Eur Radiol* 27:5272–5279
31. Becker AS, Wagner MW, Wurnig MC, Boss A (2017) Diffusion-weighted imaging of the abdomen: Impact of b-values on texture analysis features. *NMR Biomed* 30
32. Perez-Morales J, Tunali I, Stringfield O et al (2020) Peritumoral and intratumoral radiomic features predict survival outcomes among patients diagnosed in lung cancer screening. *Sci Rep* 10:10528
33. Jin X, Ai Y, Zhang J et al (2020) Noninvasive prediction of lymph node status for patients with early-stage cervical cancer based on radiomics features from ultrasound images. *Eur Radiol* 30:4117–4124
34. Shen WC, Chen SW, Liang JA, Hsieh TC, Yen KY, Kao CH (2017) [18F]Fluoro-deoxyglucose positron emission tomography for the textural features of cervical cancer associated with lymph node metastasis and histological type. *Eur J Nucl Med Mol Imaging* 44:1721–1731

Publisher's Note

Springer Nature remains neutral with regard to jurisdictional claims in published maps and institutional affiliations.

Submit your manuscript to a SpringerOpen® journal and benefit from:

- Convenient online submission
- Rigorous peer review
- Open access: articles freely available online
- High visibility within the field
- Retaining the copyright to your article

Submit your next manuscript at ► [springeropen.com](https://www.springeropen.com)